Abdominal Radiology (2019) 44:2809–2821
https://doi.org/10.1007/s00261-019-02049-5

PANCREAS

# Magnetic resonance imaging as a non-invasive method for the assessment of pancreatic fibrosis (MINIMAP): a comprehensive study design from the consortium for the study of chronic pancreatitis, diabetes, and pancreatic cancer

**Temel Tirkes[1] · Dhiraj Yadav[2] · Darwin L. Conwell[3] · Paul R. Territo[4] · Xuandong Zhao[4] · Sudhakar K. Venkatesh[5] · Arunark Kolipaka[6] · Liang Li[7] · Joseph R. Pisegna[8] · Stephen J. Pandol[9] · Walter G. Park[10] · Mark Topazian[11] · Jose Serrano[12] · Evan L. Fogel[13] on behalf of the Consortium for the Study of Chronic Pancreatitis, Diabetes, and Pancreatic Cancer**

Published online: 14 May 2019


## Abstract

Characteristic features of chronic pancreatitis (CP) may be absent on standard imaging studies. Quantitative Magnetic Resonance Imaging (MRI) techniques such as $T_1$ mapping, extracellular volume (ECV) fraction, diffusion-weighted imaging (DWI) with apparent diffusion coefficient map (ADC), MR elastography (MRE), and $T_1$-weighted signal intensity ratio (SIR) have shown promise for the diagnosis and grading severity of CP. However, radiologists still use the Cambridge classification which is based on traditional ductal imaging alone. There is an urgent need to develop new diagnostic criteria that incorporate both parenchymal and ductal features of CP seen by MRI/MRCP. Designed to fulfill this clinical need, we present the MINIMAP study, which was funded in September 2018 by the National Institutes of Health. This is a comprehensive quantitative MR imaging study which will be performed at multiple institutions in well-phenotyped CP patient cohorts. We hypothesize that quantitative MRI/MRCP features can serve as valuable non-invasive imaging biomarkers to detect and grade CP. We will evaluate the role of $T_1$ relaxometry, ECV, $T_1$-weighted gradient echo SIR, MRE, arteriovenous enhancement ratio, ADC, pancreas volume/atrophy, pancreatic fat fraction, ductal features, and pancreatic exocrine output following secretin stimulation in the assessment of CP. We will attempt to generate a multi-parametric pancreatic tissue fibrosis (PTF) scoring system. We anticipate that a quantitative scoring system may serve as a biomarker of pancreatic fibrosis; hence this imaging technique can be used in clinical practice as well as clinical trials to evaluate the efficacy of agents which may slow the progression or reverse measures of CP.

**Keywords** Chronic pancreatitis · MRI · MRCP · $T_1$ mapping · Extracellular volume · Diffusion-weighted imaging · MR elastography

## Abbreviations

| | |
|---|---|
| ADC | Apparent diffusion coefficient |
| CP | Chronic pancreatitis |
| CPDPC | Chronic pancreatitis, diabetes, and pancreatic cancer consortium |
| DWI | Diffusion-weighted imaging |
| ECV | Extracellular Volume |
| ERCP | Endoscopic retrograde cholangiopancreatography |
| MINIMAP | Magnetic resonance imaging as a non-invasive method for the assessment of pancreatic fibrosis |
| MRCP | Magnetic resonance cholangiopancreatography |
| MRI | Magnetic resonance imaging |
| MRE | Magnetic resonance elastography |
| PROCEED | Prospective evaluation of chronic pancreatitis for epidemiologic and translational studies |
| SIR | Signal intensity ratio |

✉ Temel Tirkes
atirkes@iu.edu

Extended author information available on the last page of the article

## Background

The histologic hallmarks of CP include fibrosis, chronic inflammation, and loss of acinar cells [1]. Characteristic features of chronic pancreatitis (CP) are often absent on standard diagnostic tests, including imaging studies. Indeed, Magnetic Resonance Cholangiopancreatography (MRCP) and/or Endoscopic Retrograde Cholangiopancreatography (ERCP) can be normal in patients with early disease, and diagnosis of early CP remains a challenge [2, 3]. Histologic diagnosis is rarely pursued, given the potential for complications (i.e., acute pancreatitis). Endoscopic ultrasound (EUS) and ERCP offer only a structural rather than a functional assessment of the pancreas and are less reliable in early CP. The sensitivity of available functional tests (fecal elastase and chymotrypsin, pancreolauryl and bentiromide tests, breath tests using radiolabeled pancreatic substrates) are inadequate in defining mild or moderate pancreatic disease [2, 4]. Serum pancreatic enzyme levels (amylase, lipase) are often normal in CP, and these may be of limited utility or clinical relevance in these patients. Endoscopic pancreatic function tests (ePFT) utilize a hormonal secretagogue such as secretin to maximally stimulate pancreatic secretion, followed by collection and analysis of the fluid, and may detect a decrease in this output long before exocrine insufficiency is manifested clinically [2]. Performance of the ePFT to date has typically been limited to tertiary referral centers, and while it has been used as a surrogate gold standard for the diagnosis of CP [2, 5], it may not be as sensitive [6]. It is much desired to have a practical, accessible, highly innovative, reproducible, and non-invasive imaging method to detect and quantify CP. The major role of the MR imaging has been to provide ductal imaging information to the clinicians in a non-invasive fashion. Several MR imaging techniques have been shown to be useful for detection of parenchymal changes seen with CP; however, there have not been widely accepted MRI-based diagnostic criteria that have emerged from these efforts that can potentially combine ductal and parenchymal imaging findings.

## Objectives

Our primary objective is to evaluate quantitative MRI imaging techniques as a non-invasive tool for evaluation of CP. We will assess several functional MR parameters which detect loss of proteinaceous content, restricted water diffusion, increased extracellular matrix, and stiffness of the parenchyma in addition to MR ductal imaging. We will evaluate the role of quantitative MR imaging metrics in differentiating patients with CP from patients with no pancreas disease. Review of recent literature data shows promise in this regard, with an increase in $T_1$ relaxation time, higher ECV, reduced SIR, reduced ADC, delayed phase enhancement, and decreased duodenal fluid volume in response to secretin stimulation seen in patients with CP. On the other hand, very limited data exist in subjects without pancreas disease as the control population. MINIMAP will enroll healthy volunteers as the control cohort and will attempt to validate the results of existing literature. Furthermore, we will combine findings on these parameters to generate a multi-parametric pancreas tissue fibrosis (PTF) score to quantify the features of pancreatic fibrosis. In the absence of histologic confirmation for CP, selection of appropriate cohorts is crucial, as described in SUBJECTS AND METHODS. Data generated from this study may potentially offer targets for use to study the outcome(s) of novel treatments.

## Subjects and methods

### Study organization

The consortium for the study of Chronic Pancreatitis, Diabetes, and Pancreatic Cancer (CPDPC), is supported by a cooperative agreement grant (DK108323) funded by the National Cancer Institute (NCI) and the National Institute of Diabetes and Digestive and Kidney Diseases (NIDDK). A major goal of the CPDPC is to improve diagnostic methods and treatment of CP, recurrent acute pancreatitis, and pancreatic cancer. The participating sites, the organizational structure of the CPDPC, and its studies are provided in a separate publication [7], and can also be found online at http://cpdpc.mdanderson.org. MINIMAP was funded by the NIDDK (R01DK116963) in September 2018 as a multi-institutional prospective ancillary study within the CPDPC.

### Study population

We will be recruiting a subset of adults who are participating in the CPDPC longitudinal cohort study on CP: Prospective Evaluation of Chronic Pancreatitis for Epidemiologic and Translational Studies (PROCEED) [8] (NCT03099850). Subjects with no pancreas disease (controls) and patients with suspected or definite CP who meet the inclusion and exclusion criteria will be approached for potential participation in MINIMAP. Eligibility criteria are defined in Table 1. Enrollment will take place at 7 consortium clinical centers: Indiana University Health (primary site hosting the core imaging lab) in Indianapolis, IN; University of Pittsburgh Medical Center in Pittsburgh, PA; Ohio State University in Columbus, OH; Mayo Clinic Campus in Rochester, MN;

**Table 1** Eligibility criteria

| |
|---|
| Inclusion criteria |
| Enrollment in the PROCEED Study |
| Willing to give written, informed consent |
| Exclusion criteria |
| Age < 18 or > 75 years |
| Weight ≥ 350 lbs |
| Evidence of dense calcific CP, as detected on any abdominal imaging study[a] |
| Presence of > 3 cm peri-pancreatic fluid collection |
| Prior documented allergy to secretin |
| History of moderate or severe allergic reaction to a gadolinium-based contrast agent |
| Pregnancy |
| Documented history of inflammatory bowel disease or vagotomy |
| Active, acute pancreatitis flare |
| Claustrophobia necessitating the use of general anesthesia for the performance of MRI/MRCP |
| Estimated glomerular filtration rate (eGFR) < 45 ml/min/1.73m2 |
| Severe COPD limiting breath-holding for MRI |
| Moderate or large volume ascites (of any etiology) |
| Known hemochromatosis |
| Known cystic fibrosis homozygosity |
| History of splenectomy |
| Patients with therapeutic body implants, specifically, pacemakers, defibrillators, or other implanted electronic devices that are not MRI-compatible will be excluded. Patients with an IVC filter, body piercing, neurosurgical clip placement, or shrapnel injury will be evaluated on an individual basis |

*eGFR* Estimated glomerular filtration rate, *COPD* Chronic obstructive pulmonary disease

[a]Presence of < 10 punctuate calcifications measuring < 3 mm is not an exclusion

Stanford University in Stanford, CA; Cedars-Sinai Medical Center and University of California at Los Angeles in Los Angeles, CA.

The CPDPC investigators agreed upon using the Cambridge classification based on MRI/MRCP and computed tomography (CT) to assess morphological changes in the pancreas, and to separate subjects into three groups, referred to as Green zone, Yellow zone, and Red zone as described below (Fig. 1). PROCEED investigators follow imaging guidelines recently published by the American Pancreatic Association [3]. These criteria are based on Cambridge classification, however adapted to use MRI/MRCP and CT to categorize the patients. A total of 180 subjects from the PROCEED study will be enrolled in one of the following:

a. Control group (Green zone; $n = 60$). These no pancreatic disease control subjects will have no personal history of pancreatic disease or upper abdominal symptoms and will qualify as American Society of Anesthesiologists (ASA) physical status class 1–2. Age and sex distribution of participants will be pre-defined to match the expected distribution of patients within suspected or definite CP groups.
b. Suspected CP group (Yellow zone; Cambridge grade 1 or 2; $n = 60$). These are subjects with indeterminate CP, one episode of acute pancreatitis in the preceding 18 months, or recurrent acute pancreatitis. This is a high-risk group for progression to definite CP and may be well suited for intervention studies aiming at slowing disease progression.
c. Definite CP (Red zone; Cambridge grade 3 or 4; $n = 60$). These are subjects with obvious morphologic features of CP. This group provides an opportunity to understand the prevalence and progression of functional and morphological changes and complications of the disease.

The rationale for assigning subjects into three groups was previously described in the PROCEED methodology paper [8]. The reporting standards and imaging guidelines for use in CPDPC studies (excluding MINIMAP) are also reported in a separate paper and will not be discussed here [9]. All subjects enrolling in PROCEED will be asked to provide blood, urine, saliva, and a stool sample per biospecimen standard operating procedures [10]. A subset will undergo a clinical or research EUS or esophagogastroduodenoscopy (EGD) during which pancreas fluid will be collected from the duodenum after injection of secretin for biomarker analysis.

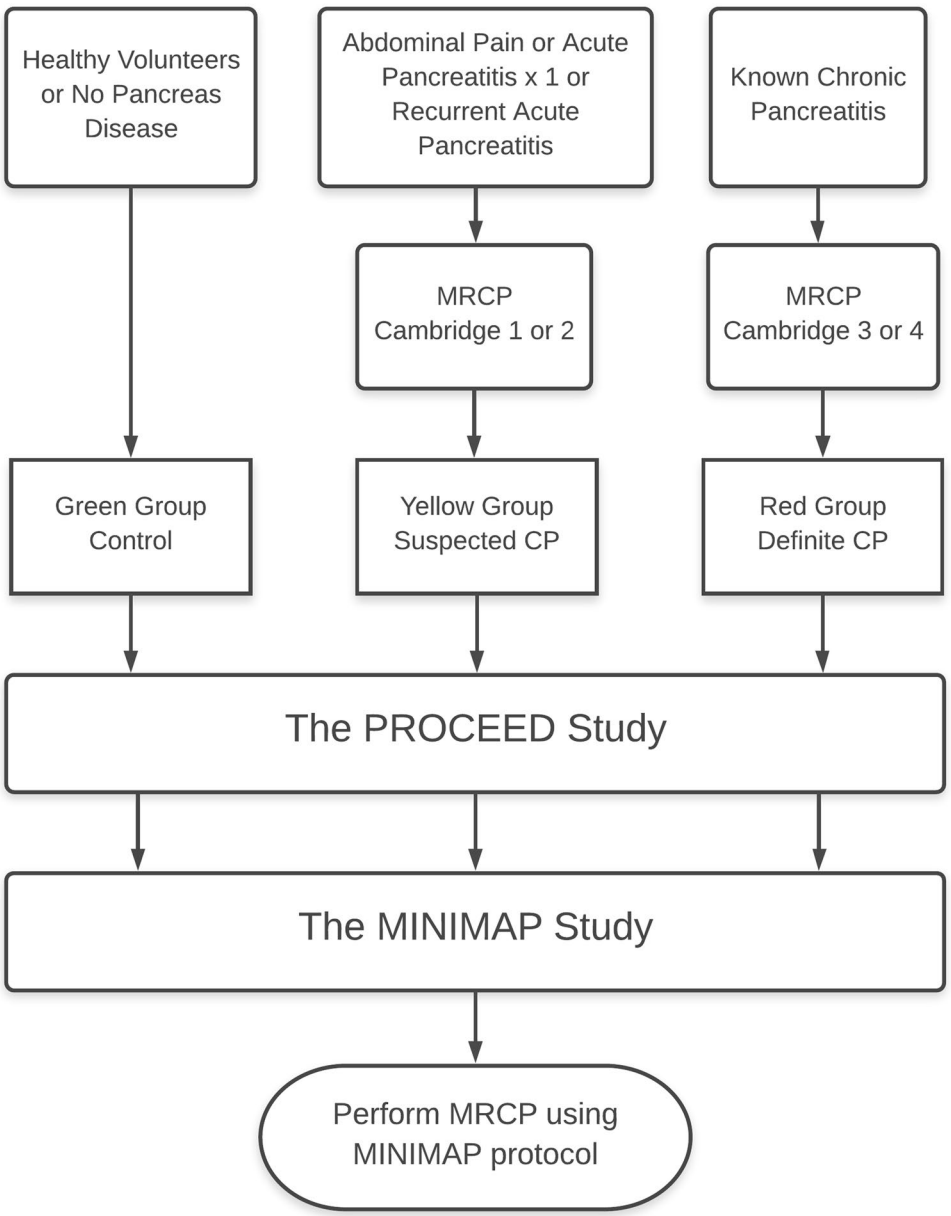


**Fig. 1** MINIMAP subject enrollment. This study will enroll subjects from the PROCEED study. Subjects will be separated into three groups, referred to as Control (Green zone), Suspected CP (Yellow zone), and Definite CP (Red zone). There will be total of 60 subjects in each group

## MR imaging

Imaging guidelines and parameters are detailed in Tables 2 and 3, respectively. MRCP will include 3D isotropic thin-slice and 2D thick-slice MRCP before and after administration of secretin (ChiRhoStim, ChiRhoClin Inc., Burtonsville, MD). $T_1$ relaxation times of tissues measured on varying magnetic signal strengths are expected to be different [11]. In this pilot study, all MRI examinations will be performed on 1.5T scanners at each study site. In a future study with a larger patient population, both 1.5T and 3T magnet strengths will be used.

All sites will acquire $T_1$ maps using dual flip-angle spoiled gradient echo (SPGR) sequence. It is necessary to standardize the quantitative imaging across different institutions and MR manufacturers using a $T_1$ phantom in order to obtain $T_1$ maps as uniform and accurately as possible. In this study, we will use a commercially available unit (System phantom model 130, High Precision Device, Inc.,) which includes an array of multiple elements. These elements are 20 mm spheres filled with solutions of $T_1$ ranging from 20 ms to 2000 ms, and $T_1$ values have been verified by the National Institute of Standards and Technology (NIST). Optimization to the dual flip-angle SPGR imaging will be made according to the phantom test results in each institution (Fig. 2). Correction for $B_1$ field inhomogeneity will be incorporated. At the present time, MRE cannot be performed at all sites due to the scarcity of required

**Table 2** MINIMAP MR imaging guidelines

| MRI/MRCP Exam Guidelines |
|---|
| 1. All imaging must be performed on a 1.5T scanner |
| 2. The imaging must be performed with torso array coils |
| 3. All patients will receive MultiHance (Gadobenate dimeglumine, Bracco Diagnostics) as MR contrast |
| 4. All patients will receive the same dosage: 0.1 mmol/kg (ml), up to 15 ml (1 vial) |
| 5. Contrast agent dosage should be same on all patients regardless of the eGFR |
| 6. Contrast agent will be injected at a rate of 2 mL/sec followed by saline flush of at least 20 mL |
| 7. Image slice thickness must be 5 mm or less |
| 8. Secretin: To adequately assess the exocrine response to secretin, patients should be fasting for at least four hours prior to the MRI exam. Fasting includes any sorts of liquids. The manufacturer's recommended dose of Secretin is 0.2 mcg/kg body weight. A test dose is no longer required by the manufacturer. 16 mcg (for adults) is administered via slow intravenous injection over one minute. Flush with 20 mL of saline |
| 9. Commercially available negative MR oral contrast is no longer available. Pineapple and blueberry juice can be used if available; however, this is not mandatory. At Indiana University Hospital, 320 ml of pineapple juice at 100% concentration has been used as a replacement |
| 10. Assess the patient's breath-holding capability. If poor, give oxygen |

**Table 3** MINIMAP MR imaging parameters

| MR imaging protocol |
|---|
| 1. Dixon series: Axial $T_1$-weighted 3-D 2-point Dixon gradient echo sequence capable of generating water-only and fat-only images in addition to in-phase and op-phase images |
| 2. Diffusion-Weighted images (DWI) and ADC map: Axial DW-SS-EPI with two b-values; 0 and 500 $mm^2$/sec; respiratory triggered |
| 3. MRCP images |
| a. 2D thick slab MRCP, 40-mm-thick, 6-8 para-coronal projections to best show the pancreatic duct from different angles |
| b. 3D MRCP: 1 mm respiratory synchronized 3-D turbo spin-echo sequence. |
| c. Secretin-stimulated 2D thick slab MRCP: After IV infusion, the ductal system is imaged via a coronal single-shot turbo spin-echo sequence, repeated every 20 s for 8 min. |
| 4. Pre-contrast $T_1$ mapping: Dual flip-angle spoiled gradient echo (SPGR) technique |
| 5. Obtain $B_1$ map (for compensation of field inhomogeneity) |
| 6. $T_1$-weighted images: 3-D gradient echo with fat suppression: a. pre-contrast b. arterial c. portal venous d. 5-minute delayed phases |
| 7. $T_2$-weighted images with fat suppression: axial |
| 8. $T_2$-weighted images: turbo spin-echo (TSE) or a variant of TSE: axial and coronal, without fat suppression |
| 9. Post-contrast $T_1$ maps |
| 10. MR elastography: MRE will be performed using a passive driver operating at 40 (or 60 Hz). Axial 3D echo planar imaging will be used to acquire images. |

Parameters may change depending on MRI hardware and optimization with phantom tests

hardware and software which is currently under development. For MRE, a 3D spin-echo echo planar imaging sequence will be employed to obtain 3D wave information along with 3D spatial data. As the pancreas is much further away from the anterior abdominal wall, shear waves at lower frequency are employed so that the shear waves reach the pancreas. Pancreas MRE at 40 Hz or 60 Hz provided more reliable stiffness values across different parts of pancreas those obtained in a pilot study with 20 normal volunteers [12] and also demonstrated the reproducibility of the technique [13]. 40 Hz is the preferred frequency for MRE of the pancreas.

## Image reconstruction

The dual flip-angle SPGR image sets will be transferred to the core imaging laboratory at Indiana University to reconstruct the $T_1$ maps using the same post-processing software (Fig. 3). To compute $T_1$ maps, SPGR images acquired using two different flip angles will be collected, imported, co-registered (to each other and $B_1$ correction map) using a normalized entropy mutual information algorithm [14], and processed according to the following equation:

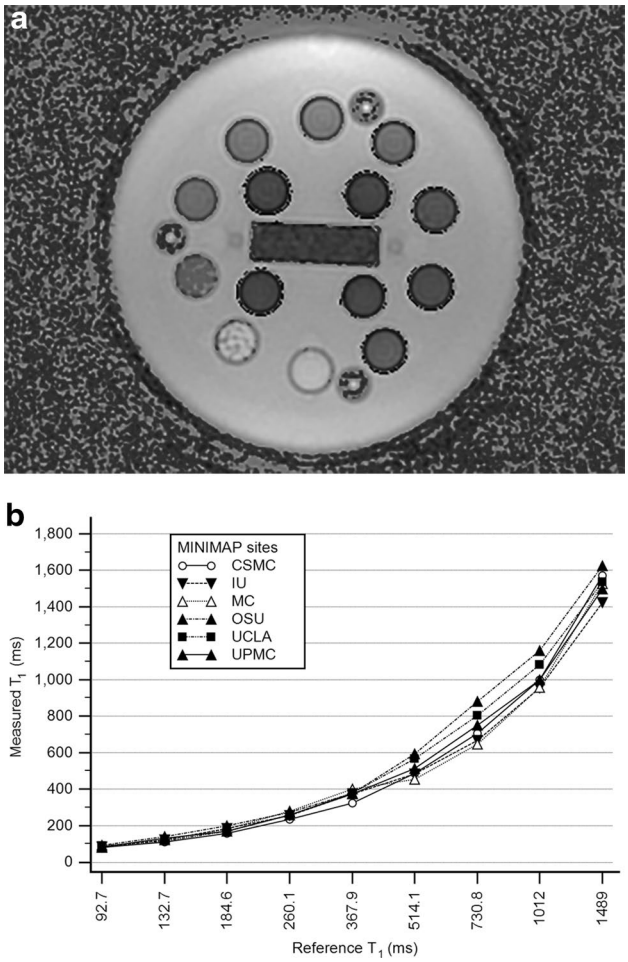


**Fig. 2** Phantom testing and protocol optimization will be performed as each institution before imaging of study subjects. **a**. This is a $T_1$ image created using the $T_1$ phantom. Each small sphere represents the measured $T_1$ of the elements within the $T_1$ phantom. The elements are 20 mm spheres filled with solutions of $T_1$ ranging from 20 ms to 2000 ms and values have been verified by the National Institute of Standards and Technology (NIST). **b**. Results of phantom testing at study sites. Optimization to the dual flip-angle SPGR parameters will be made for each institution according to the phantom test results

$T_1$ relaxation times obtained from the pancreas and the aortic lumen (blood pool) in unenhanced and 6-min delayed contrast-enhanced phases will be used to calculate the ECV fraction using the formula

$$\mathrm{ECV}_{\mathrm{pancreas}} = \frac{(1 - \mathrm{hematocrit}) \times \Delta \mathrm{R1}_{\mathrm{pancreas}}}{\Delta \mathrm{R1}_{\mathrm{blood}}},$$

where $\Delta R1_{pancreas}$ and $\Delta R1_{blood}$ are defined as the change of $1/T_1$ relaxation rate in pancreas and blood pool relaxivity before and after contrast administration, $T_1$ is a time constant describing the longitudinal relaxation rate, and its reciprocal ($1/T_1$) is referred to as R1 (Fig. 4). The change in R1 ($\Delta$R1) is defined as $\Delta R1 = (R1_{post\text{-}contrast}) - (R1_{pre\text{-}contrast})$. $\Delta$R1 is proportional to Gadolinium (Gd) concentration when both tissues are in equilibrium: $\Delta R1_{pancreas}/\Delta R1_{blood} = [Gd]_{pancreas}/[Gd]_{blood}$. Since the gadolinium chelates, such as Gd-BOPTA, are extracellular agents, the ratio of contrast agent concentrations between the pancreas and blood equals the ratio of extracellular volume between the tissues: $[Gd]_{pancreas}/[Gd]_{blood} = ECV_{pancreas}/ECV_{blood}$. The ECV of the blood is defined as the fraction of the blood volume which is not composed of blood cells (i.e., the fraction of plasma). The plasma volume is simply calculated as $ECV_{blood} = [1 - \mathrm{hematocrit}]$. Hematocrit level will be obtained on the day of MR examination if a recent test result is not available. In MRE, the obtained wave images will be directionally and bandpass filtered to remove longitudinal and reflected waves. Then the filtered wave images will be inverted to obtain spatial stiffness maps of the pancreas as shown in Fig. 5.

## Image analysis and data collection

MRCP ductal findings will be recorded by an experienced radiologist using the Cambridge classification as the diagnostic standard [17]. An experienced research analyst will perform MR data collection following delineating the contours of the pancreas at multiple levels in a semi-automated fashion using 3D volumetric image analysis software (Ana-

$$T_1\ \mathrm{map}^*(x,y,z) = -\mathrm{TR}/\ln\left(\frac{\left[\frac{I_{\mathrm{FA}_1}(x,y,z)}{\sin\left(\mathrm{FA}_1 * B_1\ \mathrm{Corr}(x,y,z)\right)} - \frac{I_{\mathrm{FA}_2}(x,y,z)}{\sin\left(\mathrm{FA}_2 * B_1\ \mathrm{corr}(x,y,z)\right)}\right]}{\left[\frac{I_{\mathrm{FA}_1}(x,y,z)}{\tan\left(\mathrm{FA}_1 * B_1\ \mathrm{corr}(x,y,z)\right)} - \frac{I_{\mathrm{FA}_2}(x,y,z)}{\tan\left(\mathrm{FA}_2 * B_1\ \mathrm{corr}(x,y,z)\right)}\right]}\right),$$

where $x$, $y$, $z$, $I_{FA_1}$, $I_{FA_2}$, TR, $FA_1$, and $FA_2$ are the horizontal position, vertical position and depth position, signal intensity of SPGR image with Flip Angle 1, signal intensity of SPGR image with Flip Angle 2, repeat time (ms), Flip Angle 1 (in radians), and Flip Angle 2 (in radians) used during the data collection [15, 16].

lyze 12.0, AnalyzeDirect, Overland Park, KS). Collected data will include $T_1$ relaxation time, $T_1$-weighted signal intensity of the (pancreas, spleen, and paraspinal muscles) in unenhanced, arterial, and 5-min delayed post-contrast phases, ADC value, stiffness of the parenchyma, pancreatic volume, diameter (in the head, body, and tail), and water and fat signal fractions using $T_1$-weighted DIXON series

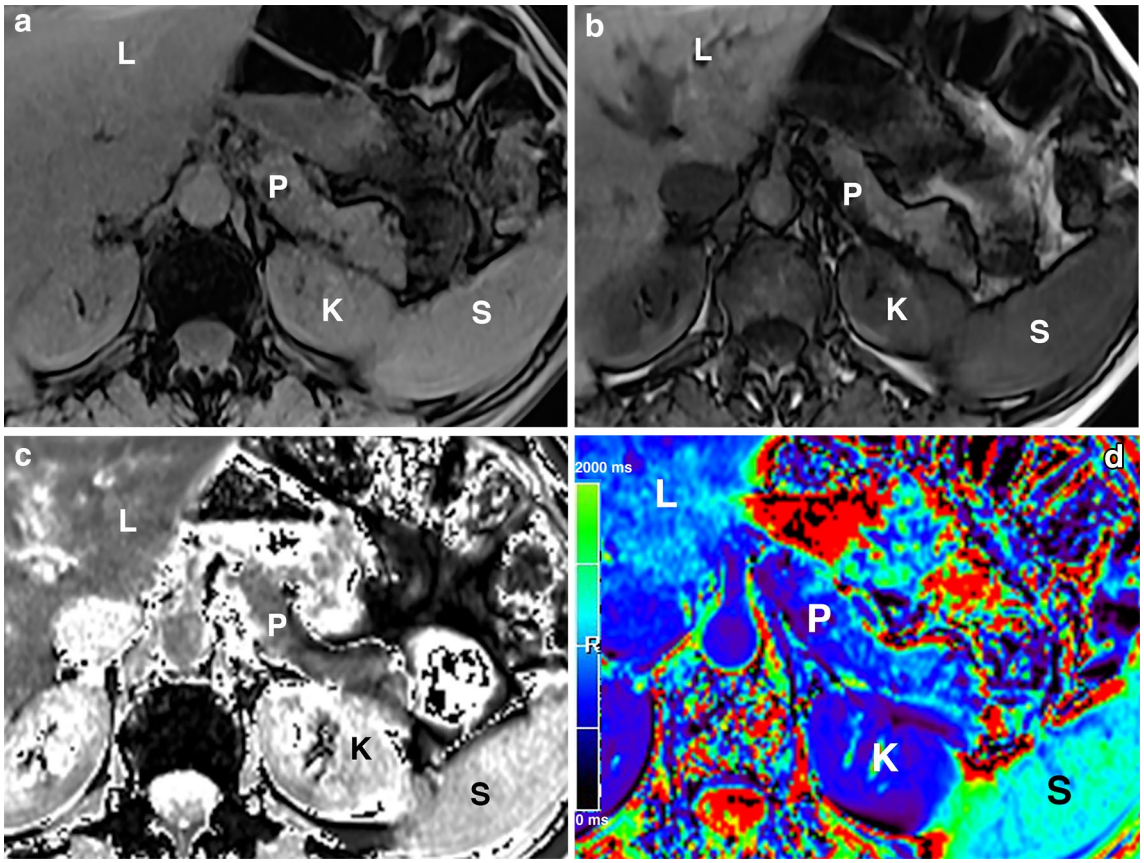


**Fig. 3** Acquisition of $T_1$ maps using dual flip-angle spoiled gradient echo (SPGR) technique. This is a 58-year-old male who presented with abdominal pain. Acquired images (**a** and **b**) will be transferred to the core imaging lab to reconstruct the $T_1$ maps (**c** and **d**). Flip angle #1 and #2 will vary depending on phantom testing performed at each institution. (*P* Pancreas, *K* Left Kidney, *L* Liver, *S* Spleen). **a**. Axial SPGR image acquired using a flip angle #1. **b**. Axial SPGR image acquired using a flip angle #2. **c**. Reconstructed $T_1$ map from the two axial SPGR images shown in Fig. 1a and b. This is a grayscale $T_1$ map on which region of interest measurements can be performed. **d**. Color $T_1$ map. $T_1$ mapping can be displayed either on grayscale or a color map. The color of the pancreas is assessed by comparing it to the color scale (from 0 to 2000 ms) seen on the left side of this image

(Table 4). While making these measurements, special attention will be given to avoid volume averaging from the signal retroperitoneal fat, dilated pancreatic duct and vessels. The signal intensity ratio of the pancreas to the spleen (SIR p/s) and signal intensity ratio of the pancreas to paraspinal muscle (SIR p/m) will be obtained by dividing the $T_1$-weighted signal intensity (SI) of the pancreas by the reference organ. $T_1$-weighted 2-point Dixon technique will be used to calculate the pancreatic fat signal fraction (FSF) by entering the SI of the pancreas on the fat-only ($SI_{Fat}$) and water-only ($SI_{Water}$) fractions into the equation: $FSF_{pancreas} = SI_{Fat}/SI_{Fat} + SI_{Water}$. The excretory volume of the pancreas will be graded on the post-secretin images of the MRCP. The duodenal filling grade will be assessed according to the degree of duodenal filling, as follows: Grade 1, pancreatic fluid is confined to the duodenal bulb; Grade 2, fluid fills the second portion of the duodenum; Grade 3, fluid fills the third portion of the duodenum; and Grade 4, fluid reaches the fourth portion of the duodenum or jejunum [18]. Visceral and subcutaneous fat content will be separated manually using image analysis software which will calculate the cross-sectional volumes of the two abdominal compartments. Visceral adipose tissue (VAT) is defined as intra-abdominal fat (including intraperitoneal and retroperitoneal fat) bound by parietal peritoneum or transversalis fascia, excluding the vertebral column and the paraspinal muscles. The subcutaneous adipose tissue (SAT) is defined as fat superficial to the abdominal and back muscles. These two fractions will be used to determine the visceral adiposity scale for each subject. Arteriovenous enhancement ratio will be obtained by the ratio of signal intensity on the arterial phase and 5-min delayed post-contrast gradient echo images. Pancreas diameter will be measured perpendicular to the main pancreatic duct in the head, body, and tail on the axial $T_1$-weighted gradient echo image with fat suppression. The pancreatic head will be measured at the thickest pancreatic head slice lying on the right side of the superior mesenteric vein. Measurement of the pancreatic body will be obtained from thickest

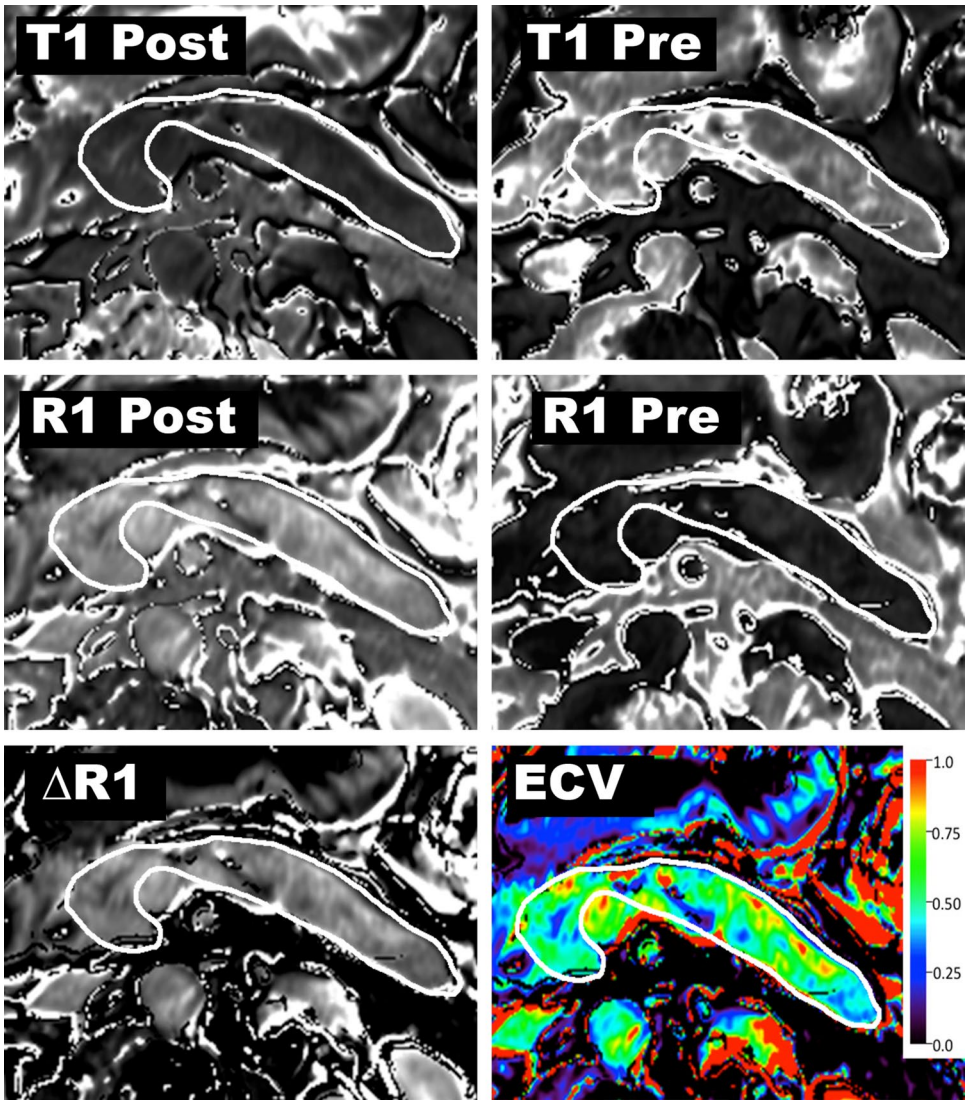


**Fig. 4** Imaging and post-processing steps for creation of an ECV map. $T_1$ relaxation times obtained from the pancreas and the aortic lumen (blood pool) in pre-contrast and 6-min delayed phases will be used to calculate the ECV fraction. $T_1$ is a time constant describing the longitudinal relaxation rate, and its reciprocal ($1/T_1$) is referred to as R1. The change in R1 is $\Delta R1 = (R1_{post\text{-}contrast}) - (R1_{pre\text{-}contrast})$. In the final step, ECV of the pancreas is calculated using $\Delta R1_{pancreas}$ and $\Delta R1_{blood}$

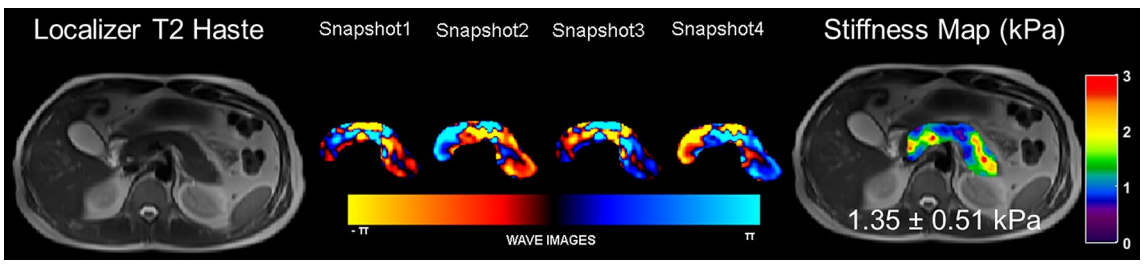


**Fig. 5** An example of MRE of the pancreas performed in a volunteer with the vibrational frequency of 60 Hz. A $T_2$ localizer along with snapshots of curl processed waves to remove the longitudinal waves along one of the encoding directions and the stiffness map overlaid on the $T_2$ localizer with a mean stiffness of 1.35 kPa in the pancreas

portion of the gland using the point of intersection between a vertical line along the left vertebral body margin and dorsal margin of the pancreas to the ventral margin of the pancreas [19]. The tail of pancreas will be measured lateral to the medial margin of the left kidney. The main pancreatic duct diameter will be subtracted from the diameter.

**Table 4** MINIMAP data collection points

| |
|---|
| $T_1$ mapping |
| Measurements will be obtained in (a) pre-contrast and (b) post-contrast equilibrium phases |
| 1. $T_1$ relaxation time of the pancreas |
| 2. $T_1$ relaxation time of the aortic lumen |
| Extracellular volume fraction |
| Measure in the head, body, tail, and the whole pancreas |
| MRCP findings |
| 1. Before secretin |
| a. Largest diameter of the main pancreatic duct |
| b. Number of ectatic side-branch ducts |
| 2. After secretin |
| a. Largest diameter of the main pancreatic duct |
| b. Number of ectatic side-branch ducts: |
| i. None |
| ii. $< 3$ |
| iii. $\geq 3$ |
| c. Ductal stricture is present |
| i. Yes (mark all that apply): head, body, tail |
| ii. No |
| d. Pancreatic ductal contour[a] |
| i. Smooth |
| ii. Mildly irregular |
| iii. Moderate to severely irregular |
| 3. Duodenal filling grade: 1, 2, 3, or 4 |
| 3D Volume of the Pancreas |
| Measure in the head, body, tail, and the whole pancreas |
| Diameter of the Pancreas |
| Measure in the head, body, and tail |
| DWI with ADC |
| Measure diffusion restriction on ADC map |
| Gradient echo $T_1$-weighted Signal of Pancreas |
| 1. Pre-contrast phase: a. pancreas, b. spleen, c. paraspinal muscle |
| 2. Post-contrast phase: a. arterial phase, b. venous phase, c. 5-minute delayed phase |
| Fat Signal Fraction (measured using $T_1$-weighted DIXON series) |
| 1. Fat-only signal of the pancreas |
| 2. Water-only signal of the pancreas |
| Abdominal Fat Distribution (measured using $T_1$-weighted DIXON series) |
| 1. Visceral adipose tissue volume |
| 2. Subcutaneous adipose tissue volume |
| MR Elastography |
| Measure stiffness in the head, body, tail, and the whole pancreas |

[a]See reference publication for details. [9]

## Statistical considerations

According to the PRoBE guidelines for biomarker development [20], we will collect pilot MRI data in 60 well-phenotyped patients with suspected CP. A similar receiver operating characteristic (ROC) analysis as in the primary objective will be conducted to compare this group with patients with definite CP. The patients with suspected CP, definite CP, and no pancreas disease controls will be compared in a descriptive analysis of patient characteristics. The patients with suspected CP are believed to be in an intermediate state during the progress to definite CP, and they may be a heterogeneous group. For the primary objective, a ROC analysis will be conducted to assess the ability of $T_1$ relaxation time to separate (discriminate) definite CP patients from controls. The rationale is that if $T_1$ is a specific biomarker for CP, it should

usually demonstrate a larger difference from the controls than other groups. We propose to assess this ability using the area under the ROC curve (AUC). We will select the quantitative MRI metrics with good discrimination ability in the ROC analysis of the primary objective and combine them to generate a composite score that further improves the discrimination ability of the MRI. The multi-parametric score will be developed based on logistic regression of disease group on multiple features. Interaction will be incorporated if justified by plausible biological mechanisms, or previous literature or improved model performance. The linear predictor of the estimated logistic regression model forms the composite score, which will be analyzed in a ROC analysis. We will use bootstrap cross-validation to guard against overestimation of AUC due to model overfitting. Based on previous publications [21, 22], we expect the AUC to be between 0.80 and 0.94. We plan to enroll 60 subjects per group, and we anticipate that ten patients per group may be excluded from analysis due to suboptimal quality of the MRI images (e.g., motion artifact, patient's intolerance, or other limitations of the study). Therefore, with 50 patients per group available for analysis, the 90% confidence interval of AUC can be estimated with a half-width between 0.06 and 0.08, when the true AUC is between 0.80 and 0.87. The half-width is smaller for a larger AUC. The results will inform the study design and sample size calculation in anticipation of a future larger population study.

## Discussion

Establishing a diagnosis of CP at an early stage has tangible benefits to the patient, but currently, this remains problematic in clinical practice. The Cambridge classification, which was originally developed for ERCP in 1984 [17], has been adopted to MRCP and has remained as the de facto diagnostic standard for decades. However, the Cambridge classification is a ductal classification system and is less sensitive for the diagnosis of early CP. Parenchymal features visualized on MRI have shown promise in establishing the CP at an early stage [23] but are not part of the current criteria. As an initial step towards establishing an MRI-based classification system, a prospective multi-institutional study is needed in well-phenotyped patients. We are presenting MINIMAP as the first comprehensive MRI study designed for this purpose.

In addition to evaluating ductal abnormalities, MRI/MRCP imaging techniques can evaluate the parenchymal changes related to fibrosis. These MR imaging techniques detect loss of proteinaceous water content, restricted water diffusion, increased stiffness, pancreatic ductal changes, and changes in the enhancement pattern of the pancreas. Due to the high protein content of the normal pancreas, the gland typically appears hyperintense on $T_1$-weighted images [24]. In CP, the normal pancreatic parenchyma rich in protein content is reduced, and the normal acinar cells become replaced by fibrosis and inflammation [25]. A decreased $T_1$ signal of the pancreas in CP reflects the degree of fibrosis and loss of normal acinar tissue, and therefore holds promise for the diagnosis of CP [21, 26]. $T_1$-weighted signal is assessed with signal intensity ratio (SIR) which compares the brightness of the pancreas to a reference organ. Decreased SIR of the pancreas has been shown to reflect the degree of fibrosis and loss of normal acinar tissue and holds promise for the diagnosis of CP [21, 26]. A recent study found a significant positive correlation between pancreatic fluid bicarbonate level and SIR of the pancreas to the spleen ($p < 0.0001$). A lower SIR of the pancreas predicted exocrine dysfunction as suggested by endoscopic pancreatic fluid collection [21]. A pancreas to splenic SIR threshold of less than 1.2 showed a sensitivity of 77% and specificity of 76% for detection of low pancreatic fluid bicarbonate, i.e., pancreatic exocrine dysfunction [21].

$T_1$ mapping is a quantitative imaging technique, which allows us to measure the tissue-specific $T_1$ relaxation time of the tissues and this may be a more reliable and accurate method compared with traditional $T_1$-weighted images. $T_1$ mapping has been used reliably to diagnose myocardial diseases [27], and has shown promise for detecting fibrosis in cirrhosis [28, 29] and CP [22, 23]. Another quantitative MR imaging method interrogates the underlying changes to the extracellular matrix that occurs during tissue fibrosis, including increases in collagen [30, 31] and proteoglycan [32] concentrations. ECV imaging dichotomizes the tissues into intra- and extracellular space and reports the extracellular fraction. A recent study performed on 119 patients showed that $T_1$ relaxation time had 64% sensitivity and 88% specificity (AUC: 0.80) for diagnosis of CP, while ECV showed 92% sensitivity and 77% specificity [22], while combining ECV and $T_1$ relaxation time yielded sensitivity of 85% and specificity of 92% (AUC: 0.94) [22]. In diffusion-weighted imaging (DWI), the signal intensity reflects the free motion or diffusion of water molecules. In fibrotic tissues, as in CP, the ADC value may be expected to decrease. In a study of 89 patients with no CP, mild CP, and severe CP (defined by MRCP using Cambridge criteria), an ADC of $< 179 \times 10$–5 $mm^2$/sec was helpful for differentiating normal pancreas from CP groups [33]. In another study, 29 patients imaged prior to pancreatectomy were found to have a pancreas-to-muscle SIR cutoff value of 1.15 on $T_1$-weighted images which yielded a sensitivity of 100% and specificity of 95% [34]. MRE of the liver has been shown to be very helpful in the evaluation of hepatic fibrosis [35]; however, MRE of the pancreas is still under development and not yet commercially available. In a pilot study, using MRE to determine pancreatic stiffness, twenty healthy volunteers underwent MRE exams using an experimental MRE

driver emitting lower frequency vibrations than those used in liver MRE imaging [12]. The mean shear stiffness (average of values obtained in different pancreatic segments) was (1.15 ± 0.17) kPa at 40 Hz and (2.09 ± 0.33) kPa at 60 Hz [12], while a different pilot study on 22 healthy volunteers showed excellent repeatability of this technique [13]. MINIMAP will verify whether MRE can provide reproducible stiffness measurements throughout the pancreas on different vendor platforms, potentially allowing for the assessment of pancreatic fibrosis in well-phenotyped patients. The consequences of pancreatic steatosis require further evaluation, and MRI allows for quantitative assessment of tissue adipose volume. In a recently published study, a moderate positive correlation between pancreatic steatosis and distribution of abdominal adipose tissue was found with the highest correlation being with the increasing adiposity within the visceral compartment ($r = 0.54$) [36]. Patients with CP showed higher visceral fat ($p = 0.01$) and pancreatic fat fraction ($p < 0.001$) indicating the presence of an association between visceral adiposity and CP. These results demonstrate the ability of MRI to quantify and correlate pancreatic steatosis; however, prospective evaluation in a larger cohort of patients is required.

In this study, a dedicated research analyst and an experienced radiologist will perform all data collection. A separate CPDPC consortium ancillary study is currently in progress evaluating inter- and intra-observer variability in the assessment of CT and MRI/MRCP findings of CP (e.g., Cambridge score, excretory volume grading, $T_1$ signal). MINIMAP was designed with predominantly quantitative imaging techniques in mind, to minimize subjective assessment. Accordingly, we expect the interobserver agreement to be satisfactory.

In conclusion, MINIMAP is the first and most comprehensive MRI study performed at multiple institutions in well-phenotyped cohorts of patients with suspected or definite CP as well as healthy subjects. This study may establish that MRI is an excellent tool for non-invasive evaluation of CP and assessment of pancreatic fibrosis. We anticipate that we will be able to develop a user-friendly multi-parametric pancreatic tissue fibrosis (PTF) scoring system. The results of MINIMAP may impact the outcome of future studies, which may identify treatments that change the natural history of CP as well as predict chronic pancreatitis progression and early pancreatic cancer.

**Acknowledgements** We acknowledge Anil Dasyam, MD; Ely Felker, MD; Zarine Shah, MD; Naoki Takahashi, MD; Shreyas Vasanawala, MD; and Ashley Wachsman, MD (in alphabetical order) for their participation in this study. We acknowledge the support of ChiRhoClin Inc. (Burtonsville, MD, USA) for supplying the Secretin (ChiRhoStim).

**Funding** Research reported in this publication was supported by National Cancer Institute and National Institute of Diabetes and Digestive and Kidney Diseases of the National Institutes of Health under award numbers R01DK116963 (MINIMAP), U01DK108323 (IU), U01DK108306 (UPMC), U01DK108327 (OSU), U01DK108314 (CSMC), DKP3041301 (UCLA), U01DK108300 (Stanford), and U01DK108288 (Mayo). The content is solely the responsibility of the authors and does not necessarily represent the official views of the National Institutes of Health.

## Compliance with ethical standards

**Conflict of interest** All authors declared that they have no competing interest.

## References

1. Kloppel G, Maillet B (1991) Chronic pancreatitis: evolution of the disease. Hepatogastroenterology 38 (5):408-412
2. Forsmark CE (2008) The early diagnosis of chronic pancreatitis. Clin Gastroenterol Hepatol 6 (12):1291-1293.
3. Conwell DL, Lee LS, Yadav D, Longnecker DS, Miller FH, Mortele KJ, Levy MJ, Kwon R, Lieb JG, Stevens T, Toskes PP, Gardner TB, Gelrud A, Wu BU, Forsmark CE, Vege SS (2014) American Pancreatic Association Practice Guidelines in Chronic Pancreatitis: evidence-based report on diagnostic guidelines. Pancreas 43 (8):1143-1162.
4. Chowdhury RS, Forsmark CE (2003) Review article: Pancreatic function testing. Aliment Pharmacol Ther 17 (6):733-750
5. Stevens T, Parsi MA (2011) Update on endoscopic pancreatic function testing. World J Gastroenterol 17 (35):3957-3961. https://doi.org/10.3748/wjg.v17.i35.3957
6. Lara LF, Takita M, Burdick JS, DeMarco DC, Pimentel RR, Erim T, Levy MF (2017) A study of the clinical utility of a 20-minute secretin-stimulated endoscopic pancreas function test and performance according to clinical variables. Gastrointest Endosc 86 (6):1048-1055 e1042. https://doi.org/10.1016/j.gie.2017.03.1532
7. Serrano J, Andersen DK, Forsmark CE, Pandol SJ, Feng Z, Srivastava S, Rinaudo JAS, Consortium for the Study of Chronic Pancreatitis D, Pancreatic C (2018) Consortium for the Study of Chronic Pancreatitis, Diabetes, and Pancreatic Cancer: From Concept to Reality. Pancreas 47 (10):1208-1212. https://doi.org/10.1097/mpa.0000000000001167
8. Yadav D, Park WG, Fogel EL, Li L, Chari ST, Feng Z, Fisher WE, Forsmark CE, Jeon CY, Habtezion A, Hart PA, Hughes SJ, Othman MO, Rinaudo JAS, Pandol SJ, Tirkes T, Serrano J, Srivastava S, Van Den Eeden SK, Whitcomb DC, Topazian M, Conwell DL, Consortium for the Study of Chronic Pancreatitis D, Pancreatic C (2018) PROspective Evaluation of Chronic Pancreatitis for EpidEmiologic and Translational StuDies: Rationale and Study Design for PROCEED From the Consortium for the Study of Chronic Pancreatitis, Diabetes, and Pancreatic Cancer. Pancreas 47 (10):1229-1238. https://doi.org/10.1097/mpa.0000000000001170
9. Tirkes T, Shah ZK, Takahashi N, Grajo JR, Chang ST, Venkatesh SK, Conwell DL, Fogel EL, Park W, Topazian M, Yadav D, Dasyam AK, Consortium for the Study of Chronic Pancreatitis D, Pancreatic C (2019) Reporting Standards for Chronic Pancreatitis by Using CT, MRI, and MR Cholangiopancreatography: The Consortium for the Study of Chronic Pancreatitis, Diabetes, and Pancreatic Cancer. Radiology 290 (1):207-215. https://doi.org/10.1148/radiol.2018181353
10. Fisher WE, Cruz-Monserrate Z, McElhany AL, Lesinski GB, Hart PA, Ghosh R, Van Buren G, Fishman DS, Rinaudo JAS, Serrano J,

Srivastava S, Mace T, Topazian M, Feng Z, Yadav D, Pandol SJ, Hughes SJ, Liu RY, Lu E, Orr R, Whitcomb DC, Abouhamze AS, Steen H, Sellers ZM, Troendle DM, Uc A, Lowe ME, Conwell DL, Consortium for the Study of Chronic Pancreatitis D, Pancreatic C (2018) Standard Operating Procedures for Biospecimen Collection, Processing, and Storage: From the Consortium for the Study of Chronic Pancreatitis, Diabetes, and Pancreatic Cancer. Pancreas 47 (10):1213-1221. https://doi.org/10.1097/mpa.0000000000001171

11. Soher BJ, Dale BM, Merkle EM (2007) A review of MR physics: 3T versus 1.5T. Magn Reson Imaging Clin N Am 15 (3):277-290, v. https://doi.org/10.1016/j.mric.2007.06.002
12. Shi Y, Glaser KJ, Venkatesh SK, Ben-Abraham EI, Ehman RL (2015) Feasibility of using 3D MR elastography to determine pancreatic stiffness in healthy volunteers. J Magn Reson Imaging 41 (2):369-375. https://doi.org/10.1002/jmri.24572
13. Kolipaka A, Schroeder S, Mo X, Shah Z, Hart PA, Conwell DL (2017) Magnetic resonance elastography of the pancreas: Measurement reproducibility and relationship with age. Magn Reson Imaging 42:1-7. https://doi.org/10.1016/j.mri.2017.04.015
14. Fitzpatrick JM, Hill DL, Shyr Y, West J, Studholme C, Maurer CR, Jr. (1998) Visual assessment of the accuracy of retrospective registration of MR and CT images of the brain. IEEE Trans Med Imaging 17 (4):571-585. https://doi.org/10.1109/42.730402
15. Boudreau M, Tardif CL, Stikov N, Sled JG, Lee W, Pike GB (2017) B1 mapping for bias-correction in quantitative T1 imaging of the brain at 3T using standard pulse sequences. J Magn Reson Imaging 46 (6):1673-1682. https://doi.org/10.1002/jmri.25692
16. Cheng HL, Wright GA (2006) Rapid high-resolution T(1) mapping by variable flip angles: accurate and precise measurements in the presence of radiofrequency field inhomogeneity. Magn Reson Med 55 (3):566-574. https://doi.org/10.1002/mrm.20791
17. Sarner M, Cotton PB (1984) Classification of pancreatitis. Gut 25(7):756–759
18. Cappeliez O, Delhaye M, Deviere J, Le Moine O, Metens T, Nicaise N, Cremer M, Stryuven J, Matos C (2000) Chronic pancreatitis: evaluation of pancreatic exocrine function with MR pancreatography after secretin stimulation. Radiology 215 (2):358-364. https://doi.org/10.1148/radiology.215.2.r00ma10358
19. Wang Q, Swensson J, Hu M, Cui E, Tirkes T, Jennings SG, Akisik F (2019) Distribution and correlation of pancreatic gland size and duct diameters on MRCP in patients without evidence of pancreatic disease. Abdom Radiol (NY). https://doi.org/10.1007/s00261-018-1879-3
20. Pepe MS, Etzioni R, Feng Z, et al. (2001) Phases of biomarker development for early detection of cancer. J Natl Cancer Inst 93(14):1054–1061
21. Tirkes T, Fogel EL, Sherman S, Lin C, Swensson J, Akisik F, Sandrasegaran K (2017) Detection of exocrine dysfunction by MRI in patients with early chronic pancreatitis. Abdom Radiol (NY) 42 (2):544-551. https://doi.org/10.1007/s00261-016-0917-2
22. Tirkes T, Lin C, Cui E, Deng Y, Territo PR, Sandrasegaran K, Akisik F (2018) Quantitative MR Evaluation of Chronic Pancreatitis: Extracellular Volume Fraction and MR Relaxometry. AJR Am J Roentgenol 210 (3):533-542. https://doi.org/10.2214/ajr.17.18606
23. Tirkes T, Lin C, Fogel EL, Sherman SS, Wang Q, Sandrasegaran K (2017) T1 mapping for diagnosis of mild chronic pancreatitis. J Magn Reson Imaging 45 (4):1171-1176. https://doi.org/10.1002/jmri.25428
24. Winston CB, Mitchell DG, Outwater EK, Ehrlich SM (1995) Pancreatic signal intensity on T1-weighted fat saturation MR images: clinical correlation. J Magn Reson Imaging 5 (3):267-271
25. Ammann RW, Heitz PU, Kloppel G (1996) Course of alcoholic chronic pancreatitis: a prospective clinicomorphological long-term study. Gastroenterology 111 (1):224-231
26. Balci NC, Smith A, Momtahen AJ, Alkaade S, Fattahi R, Tariq S, Burton F (2010) MRI and S-MRCP findings in patients with suspected chronic pancreatitis: correlation with endoscopic pancreatic function testing (ePFT). J Magn Reson Imaging 31 (3):601-606. https://doi.org/10.1002/jmri.22085
27. Schelbert EB, Messroghli DR (2016) State of the Art: Clinical Applications of Cardiac T1 Mapping. Radiology 278 (3):658-676. https://doi.org/10.1148/radiol.2016141802
28. Kim KA, Park MS, Kim IS, Kiefer B, Chung WS, Kim MJ, Kim KW (2012) Quantitative evaluation of liver cirrhosis using T1 relaxation time with 3 tesla MRI before and after oxygen inhalation. J Magn Reson Imaging 36 (2):405-410. https://doi.org/10.1002/jmri.23620
29. Luetkens JA, Klein S, Traber F, Schmeel FC, Sprinkart AM, Kuetting DLR, Block W, Uschner FE, Schierwagen R, Hittatiya K, Kristiansen G, Gieseke J, Schild HH, Trebicka J, Kukuk GM (2018) Quantification of Liver Fibrosis at T1 and T2 Mapping with Extracellular Volume Fraction MRI: Preclinical Results. Radiology 288 (3):748-754. https://doi.org/10.1148/radiol.2018180051
30. Haber PS, Keogh GW, Apte MV, Moran CS, Stewart NL, Crawford DH, Pirola RC, McCaughan GW, Ramm GA, Wilson JS (1999) Activation of pancreatic stellate cells in human and experimental pancreatic fibrosis. Am J Pathol 155 (4):1087-1095. https://doi.org/10.1016/s0002-9440(10)65211-x
31. Charrier AL, Brigstock DR (2010) Connective tissue growth factor production by activated pancreatic stellate cells in mouse alcoholic chronic pancreatitis. Lab Invest 90 (8):1179-1188. https://doi.org/10.1038/labinvest.2010.82
32. Pan S, Chen R, Stevens T, Bronner MP, May D, Tamura Y, McIntosh MW, Brentnall TA (2011) Proteomics portrait of archival lesions of chronic pancreatitis. PLoS One 6 (11):e27574. https://doi.org/10.1371/journal.pone.0027574
33. Akisik MF, Aisen AM, Sandrasegaran K, Jennings SG, Lin C, Sherman S, Lin JA, Rydberg M (2009) Assessment of chronic pancreatitis: utility of diffusion-weighted MR imaging with secretin enhancement. Radiology 250 (1):103-109. https://doi.org/10.1148/radiol.2493080160
34. Watanabe H, Kanematsu M, Tanaka K, Osada S, Tomita H, Hara A, Goshima S, Kondo H, Kawada H, Noda Y, Tanahashi Y, Kawai N, Yoshida K, Moriyama N (2014) Fibrosis and postoperative fistula of the pancreas: correlation with MR imaging findings–preliminary results. Radiology 270 (3):791-799. https://doi.org/10.1148/radiol.13131194
35. Wang Y, Ganger DR, Levitsky J, Sternick LA, McCarthy RJ, Chen ZE, Fasanati CW, Bolster B, Shah S, Zuehlsdorff S, Omary RA, Ehman RL, Miller FH (2011) Assessment of chronic hepatitis and fibrosis: comparison of MR elastography and diffusion-weighted imaging. Am J Roentgenol 196 (3):553-561. https://doi.org/10.2214/ajr.10.4580
36. Tirkes T, Jeon CY, Li L, Joon AY, Seltman TA, Sankar M, Persohn SA, Territo PR (2019) Association of Pancreatic Steatosis With Chronic Pancreatitis, Obesity, and Type 2 Diabetes Mellitus. Pancreas. https://doi.org/10.1097/mpa.0000000000001252

## Affiliations

**Temel Tirkes[1] · Dhiraj Yadav[2] · Darwin L. Conwell[3] · Paul R. Territo[4] · Xuandong Zhao[4] · Sudhakar K. Venkatesh[5] · Arunark Kolipaka[6] · Liang Li[7] · Joseph R. Pisegna[8] · Stephen J. Pandol[9] · Walter G. Park[10] · Mark Topazian[11] · Jose Serrano[12] · Evan L. Fogel[13] on behalf of the Consortium for the Study of Chronic Pancreatitis, Diabetes, and Pancreatic Cancer**

1 Department of Radiology and Imaging Sciences, Indiana University School of Medicine, 550N. University Blvd. Suite 0663, Indianapolis, IN 46202, USA

2 Division of Gastroenterology, Hepatology & Nutrition, Department of Medicine, University of Pittsburgh School of Medicine, Pittsburgh, PA, USA

3 Department of Medicine, Division of Gastroenterology, Hepatology & Nutrition, Ohio State University Wexner Medical Center, Columbus, OH, USA

4 Department of Radiology and Imaging Sciences, Indiana University School of Medicine, 950 W. Walnut Street, R2 E124G, Indianapolis, IN 46202, USA

5 Department of Radiology, Mayo Clinic, Rochester, MN, USA

6 The Ohio State University Wexner Medical Center, 395 West 12th AVE, 4th Floor, Columbus, OH 43210, USA

7 Department of Biostatistics, The University of Texas MD Anderson Cancer Center, Houston, TX, USA

8 Division of Gastroenterology and Hepatology, Departments of Medicine and Human Genetics, VA Greater Los Angeles HCS, Los Angeles, CA, USA

9 Division of Digestive and Liver Diseases, Cedars-Sinai Medical Center, Los Angeles, CA, USA

10 Division of Gastroenterology and Hepatology, Department of Medicine, Stanford University Medical Center, Stanford, CA, USA

11 Division of Gastroenterology and Hepatology, Department of Medicine, Mayo Clinic Campus, Rochester, MN, USA

12 CAPT, Medical Corps US Public Health Service, Division of Digestive Diseases and Nutrition, National Institute of Diabetes and Digestive and Kidney Diseases, 2 Democracy Plaza, Room 6007, MSC 5450, Bethesda, MD 20892, USA

13 Lehman, Bucksot and Sherman Section of Pancreatobiliary Endoscopy, Indiana University School of Medicine, Indianapolis, IN, USA